C. R. Chimie 22 (2019) 84–95

Contents lists available at ScienceDirect

Comptes Rendus Chimie

www.sciencedirect.com

Full paper/Mémoire

Synthesis of recoverable palladium composite as an efficient catalyst for the reduction of nitroarene compounds and Suzuki cross-coupling reactions using sepiolite clay and magnetic nanoparticles (Fe_3O_4@sepiolite-Pd^{2+})

Ehsan Ghonchepour [a, *], Mohammad Reza Islami [a, **], Behjat Bananezhad [a], Hamid Mostafavi [b], Ahmad Momeni Tikdari [a]

[a] Department of Chemistry, Shahid Bahonar University of Kerman, 22 Bahman Avenue, 76169 Kerman, Iran
[b] Kerman Agricultural and Natural Resource Research and Education Center, AREEO, Kerman, Iran

ARTICLE INFO

Article history:
Received 26 April 2018
Accepted 23 July 2018
Available online 19 November 2018

Keywords:
Palladium
Sepiolite clay
Magnetic nanoparticles
Heterogenization
C–C coupling
Green catalyst
Suzuki reaction

ABSTRACT

Clays are nontoxic, inexpensive, abundant, and have great potential as catalytic carriers because of their special structure, surface, and suitability for supporting transition metals. In this study, sepiolite was used as a ligand for the heterogenization of palladium chloride on Fe_3O_4 nanoparticle surface as a novel, high temperature stable, and recoverable green catalyst (Fe_3O_4@sepiolite-Pd^{2+}). The catalytic activity of this system was tested in the reduction of nitroarene compounds and the Suzuki cross-coupling reaction. The catalyst structure was characterized using spectroscopic data and magnetic and thermal techniques such as Fourier transform infrared, scanning electron microscopy, energy-dispersive X-ray spectroscopy (EDX), X-ray diffraction, vibrating sample magnetometer (VSM), and thermogravimetric analysis.

1. Introduction

Since the beginning of human history, soils have been the most available and cheapest materials used by humans, and still, our lives are inevitably dependent upon the availability of soils.

From constructing shelters to producing consumable goods, soils are useful materials for many purposes, including pharmaceutical and industrial applications [1–3]. There are many different categories of soils, each having unique characteristics regarding color, texture, structure, and contents. Clay is the most important category of soils. It contributes a great deal to industry and our lives. Different minerals constitute clay [4]. Clay particles have a diameter of less than 0.002 mm.

Among the minerals in clay, sepiolite is one of the most important. It consists of hydrated magnesium silicate and has the potential to be a catalytic carrier because of its special structure. The formula of sepiolite as a fibrous natural clay mineral is $[Si_{12}Mg_8O_{30}(OH)_4 \cdot 8H_2O]$. The structure of sepiolite consists of layers of silicate that are connected by magnesium ions, as in mica. Every Si is tetrahedrally surrounded by four oxygen atoms. The Mg ions are surrounded octahedrally by oxygen atoms and

* Corresponding author.
** Corresponding author.
E-mail addresses: ghonchepoor@gmail.com (E. Ghonchepour), mrislami@uk.ac.ir (M.R. Islami).

https://doi.org/10.1016/j.crci.2018.07.008

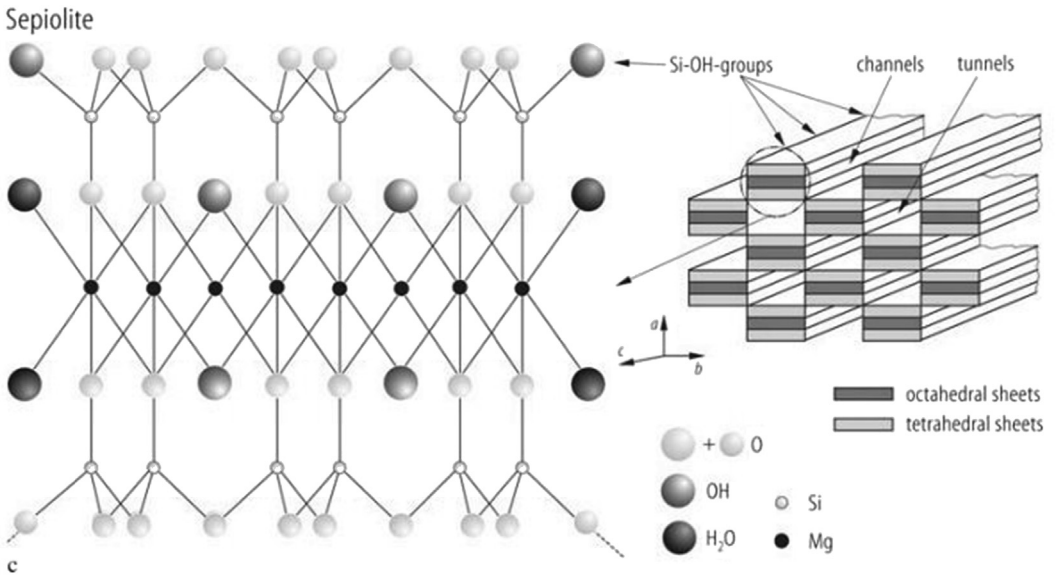

Fig. 1. Structure of sepiolite.

hydroxyl groups, and the coordination of each Mg at the end of the complex involves 2H—O molecules (Fig. 1) [5,6].

Literature mining revealed that sepiolites react with NaOH at 110 °C in an autoclave. Therefore, the Mg^{2+} ions at the edges of the sepiolite channels are replaced by Na^{+} ions. Sepiolite contains Na^{+} that can easily be exchanged by transition metal ions or any other alkali ions [7,8].

The design and use of environmentally safe catalysts as a key component of green chemistry is an important challenge to industry [9,10]. Some of the essential characteristics of a green catalyst are high activity, high stability, selectivity, easy and efficient recoverability, low preparation cost, and good recyclability [11]. In this context, more attention is given on homogeneous catalysts as compared to heterogeneous approaches. The use of homogeneous catalysts in industry has been problematic because of the difficult separation, the toxicity of such catalysts, and the loss of catalyst activity after one run [12]. To avoid these problems, a heterogeneous catalytic system has recently been extensively used in various synthetic transformations. Straightforward experimental procedures, mild reaction conditions, the reusability of catalysts, and minimal waste disposal are the most important advantages of heterogeneous systems [13].

A useful group of heterogeneous systems is the magnetic-supported catalysts, which can be separated using an external magnetic field. Such catalysts could have a longer life and minimize the changes in activity and selectivity as compared with homogeneous catalysts [14,15]. A surface may be synthesized with the properties of magnetic nanoparticles using different methods, such as (1) covering the surface with oxides, carbon, polymer, or metallic layers; (2) the noncovalent approach with polymers or surfactants; or (3) the covalent approach between hydroxyl groups on the nanoparticles' surface and anchoring agents such as carboxylic acid, phosphoric acid, and dopamine derivatives [14].

2. Experimental section

2.1. Chemicals

All solvents and chemicals (analytical grades) were purchased and used without further purification. Palladium(II) chloride (99.9%) was purchased from the Merck Company. Fourier transform infrared (FT-IR) spectra were obtained in an area of 400—4000 cm^{-1} using a Nicolet IR100 instrument with spectroscopic grade KBr. The images and EDX analyses of the catalyst were observed using gold-coated Philips XL 30 and S-4160 instruments equipped with dispersive X-ray spectroscopy capabilities. Thermogravimetric analysis was performed on a thermal analyzer with a heating rate of 10 °C min^{-1} over a temperature region of 25—600 °C under flowing compressed nitrogen gas. Powder X-ray diffraction (XRD) spectra were recorded at room temperature using a Philips X-Pert 1710 diffractometer and Co Kα (λ= 1.78897 Å) at a voltage of 40 kV and current of 40 mA. Data were collected from 10° to 90° (2θ) with a scan speed of 0.02° s^{-1}. The magnetic properties of the catalyst nanoparticles were obtained using a vibrating magnetometer/alternating gradient force magnetometer. The morphology of the catalyst was studied using scanning electron microscopy (SEM; Zeiss SIGMA VP) and transmission electron microscopy (TEM; Zeiss-EM10C-100 kV).

2.2. Preparation of sepiolite-coated magnetic nanoparticles (Fe_3O_4@sepiolite)

To prepare the sepiolite magnetic nanoparticles (Fe_3O_4@sepiolite), a mixture of 1 g sepiolite was dispersed

in 50 mL deionized water and stirred for 4 h in an ultrasonic bath. This suspension was added to a mixture of 0.994 g (5 mmol) $FeCl_2 \cdot 4H_2O$ and 2.7 g (10 mmol) $FeCl_3 \cdot 6H_2O$ salts, which were dissolved in 100 mL of deionized water under intense stirring. An aqueous ammonia solution (30 mL) (25% w/w) was added to the resultant mixture to increase the reaction pH to about 11. The mixture was stirred at 80 °C for 1 h. After cooling to room temperature, the sepiolite-coated magnetic nanoparticle composites were collected with an external magnet, washed three times in hot water, and dried at 100 °C for 12 h.

2.3. Synthesis of palladium ion encapsulated with sepiolite-coated magnetic nanoparticles (Fe_3O_4@sepiolite-Pd^{2+})

Palladium chloride 177 mg (1 mmol) was added to 1 g Fe_3O_4@sepiolite in 50 mL deionized water, and the mixture was stirred at room temperature for 24 h. Subsequently, the final composite was separated with an external magnet, washed three times with deionized water, and dried at 80 °C for 12 h (Scheme 1).

2.4. General procedure for reduction of nitroarenes in the presence of Fe_3O_4@sepiolite-Pd^{2+}

To the stirred mixture of nitroarene compound (1 mmol) in 4 mL EtOH/H_2O (3:1), 5 mmol $NaBH_4$ (0.189 g) and 20 mg of Fe_3O_4@sepiolite-Pd^{2+} were added. The reaction vessel was heated at 70 °C in an oil bath for 10–50 min. The progress of the reaction was scanned by thin-layer chromatography (TLC). After completion of the reaction, the nanoparticles were separated from the reaction mixture by an external magnet and washed repeatedly with deionized water and diethyl ether. Water (50 mL) was then added to the reaction mixture, extracted with CH_2Cl_2 (2 × 20 mL), and dried over Na_2SO_4. The solvent was removed under reduced pressure, and the products were purified with silica-gel plate chromatography using *n*-hexane–ethyl acetate as an eluent to afford pure product.

2.5. General procedure for the Suzuki coupling reaction in the presence of Fe_3O_4@sepiolite-Pd^{2+}

Aryl halide compound (1 mmol) and K_2CO_3 (2 mmol) in EtOH/H_2O (1:1, 8 mL) and 10 mg of Fe_3O_4@sepiolite-Pd^{2+} were added to a stirred mixture of phenylboronic acid (1 mmol). The mixture was then heated and stirred at 70 °C for 15 min. The progress of the reaction was monitored by TLC. After completion of the reaction, the nanoparticles were separated from the reaction mixture with an external magnet and washed repeatedly with deionized water and diethyl ether. Water (50 mL) was then added to the reaction mixture, extracted with CH_2Cl_2 (2 × 20 mL), and dried over Na_2SO_4. The solvent was removed under reduced pressure, and the products were purified using a column chromatography eluted with *n*-hexane. The solvent was removed to give pure product.

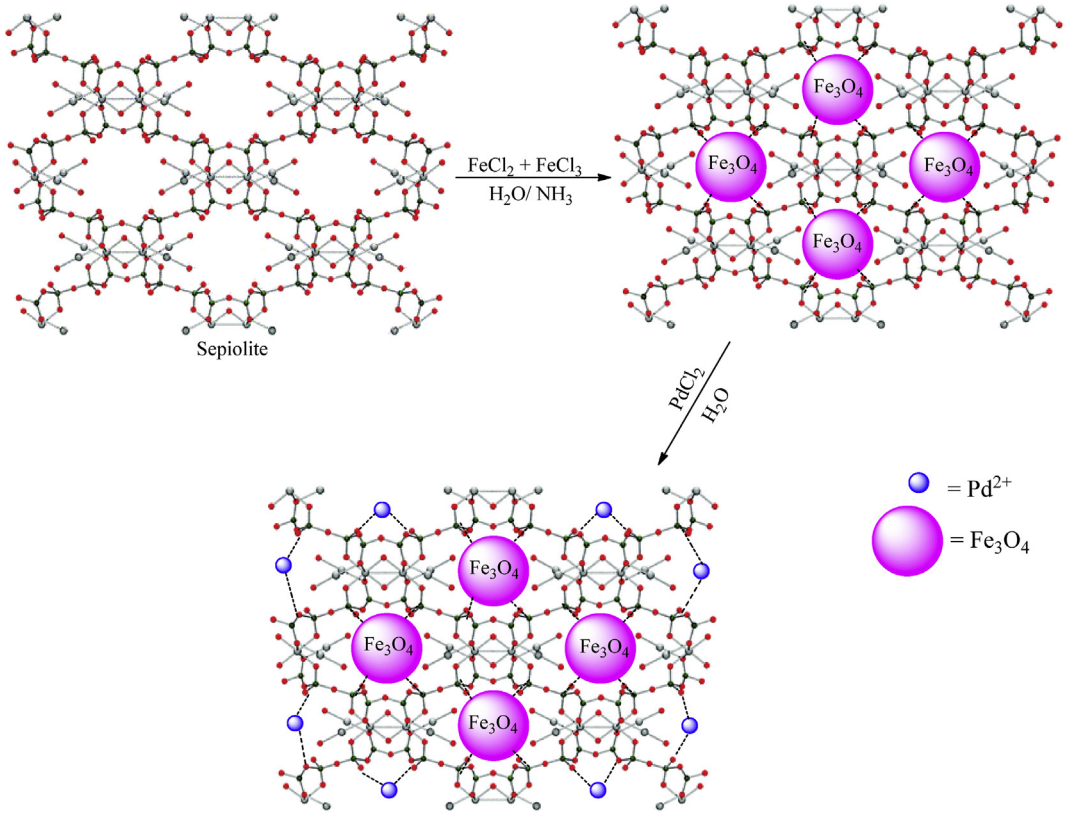

Scheme 1. Synthesis of Fe_3O_4@sepiolite-Pd^{2+}.

3. Results and discussion

3.1. Characterization of Fe_3O_4@sepiolite-Pd^{2+}

The FT-IR spectrum of sepiolite (a), Fe_3O_4@sepiolite (b), and Fe_3O_4@sepiolite-Pd^{2+} (c) is depicted in Fig. 2. The spectrum of pristine sepiolite is shown in Fig. 2(a). The absorption bands at 3686 and 3562 cm^{-1} correspond to the OH groups of Mg_3OH. The stretching vibration at 1658 cm^{-1} can be attributed to the water of zeolite, and the bands at the 1015 and 470 cm^{-1} can be assigned as the Si—O—Si vibration [16]. Fig. 2(b) shows the FT-IR spectrum of sepiolite-supported magnetic nanoparticles (Fe_3O_4@sepiolite). The typical bands that appear at 400–600 cm^{-1} are caused by the Fe—O stretching vibration. The absorption band at 3562 cm^{-1} in the IR spectrum of sepiolite is replaced by a broadband at 3441 cm^{-1}, which is because of the stretching vibrations of the hydroxyl groups in Fe_3O_4 and water. This shift proves the binding of a sepiolite to the surface of Fe_3O_4 nanoparticles through the chemisorption of the hydroxyl group [17].

The FT-IR spectrum of the final composite (Fe_3O_4@sepiolite-Pd^{2+}), which was prepared from the stabilization of $PdCl_2$ on Fe_3O_4@sepiolite, is indicated in Fig. 2(c). The hydroxyl group stretching frequency is shifted to a lower frequency at 3418 cm^{-1}, indicating that the OH bond is coordinated with the palladium. All of the absorption bands in the final catalyst shifted to lower frequencies, thus confirming that the Pd ion was placed on the magnetic composite.

Fig. 3 shows the thermogravimetric analysis of Fe_3O_4@sepiolite-Pd^{2+}. This analysis was recorded by heating the sample at a rate of 10 °C min^{-1}. The endothermic peak at lower temperatures (lower than 110 °C) can be attributed to the desorption of physically absorbed water on the surface of sepiolite and Fe_3O_4. This analysis indicates that the 1.03% weight loss in the range of 250–310 °C can be ascribed to the water loss in this area [18]. Therefore, this composite is stable at 600 °C, and according to this analysis, the Fe_3O_4@sepiolite-Pd^{2+} composite is a high-temperature stable catalyst. The amount of metal supported onto the Fe_3O_4@sepiolite was measured by induced coupled plasma analysis, and the amount of Pd was 0.032 g per gram of catalyst (0.3 mmol g^{-1}).

The hysteresis loop for Fe_3O_4@sepiolite-Pd^{2+} in an applied magnetic field at ambient temperatures was studied with the field swept from −8000 to +8000 Oe (Fig. 4). Bare nanocrystals of Fe_3O_4 have the high saturation magnetization of 73.7 emu g^{-1} at room temperature [19]. This magnetization decreases to 34 emu g^{-1} in the Fe_3O_4@sepiolite-Pd^{2+} catalyst, which demonstrates that the nanoparticles exhibit high permeability in magnetization. Thus, it is sufficient for magnetic separation using a conventional magnet.

Fig. 5(a) and (b) shows the SEM and TEM images of the Fe_3O_4@sepiolite-Pd^{2+}. SEM images confirm the presence of spherical nanoparticles with a rough surface in the 23–58 nm diameter range (Fig. 5(a)). Transmission electron microscopy (TEM) confirmed the formation of single-phase Fe_3O_4 nanoparticles with spherical morphology (Fig. 5(b)).

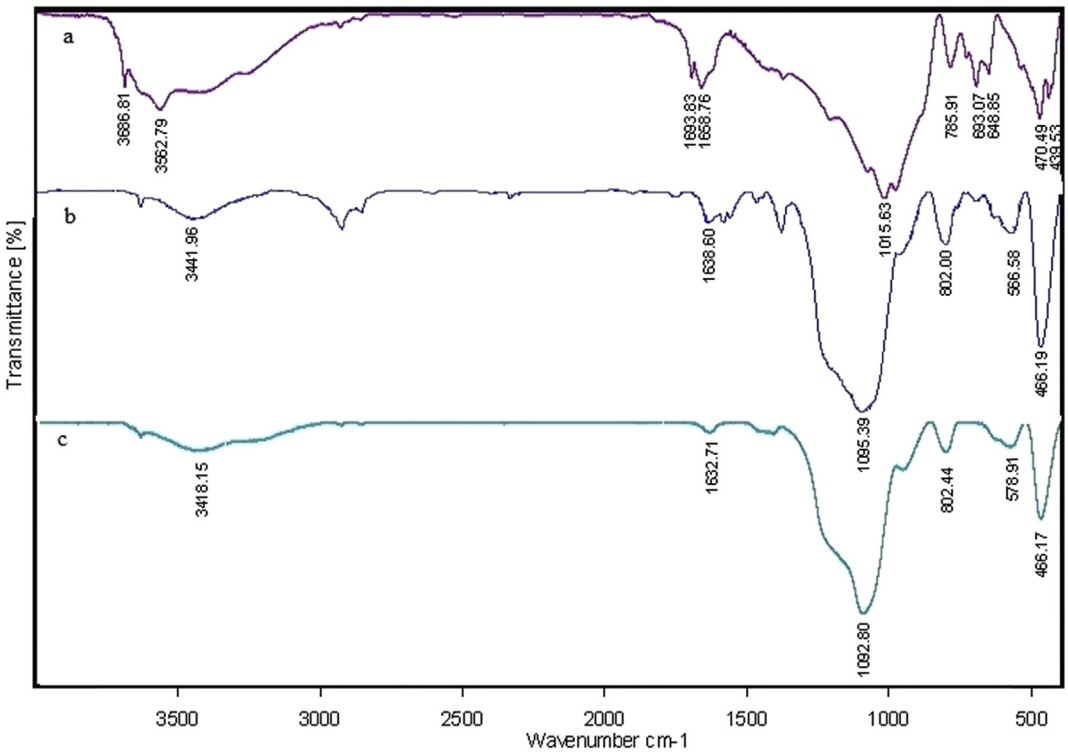

Fig. 2. The FT-IR spectrum of sepiolite (a), Fe_3O_4@sepiolite (b), and Fe_3O_4@sepiolite-Pd^{2+} (c).

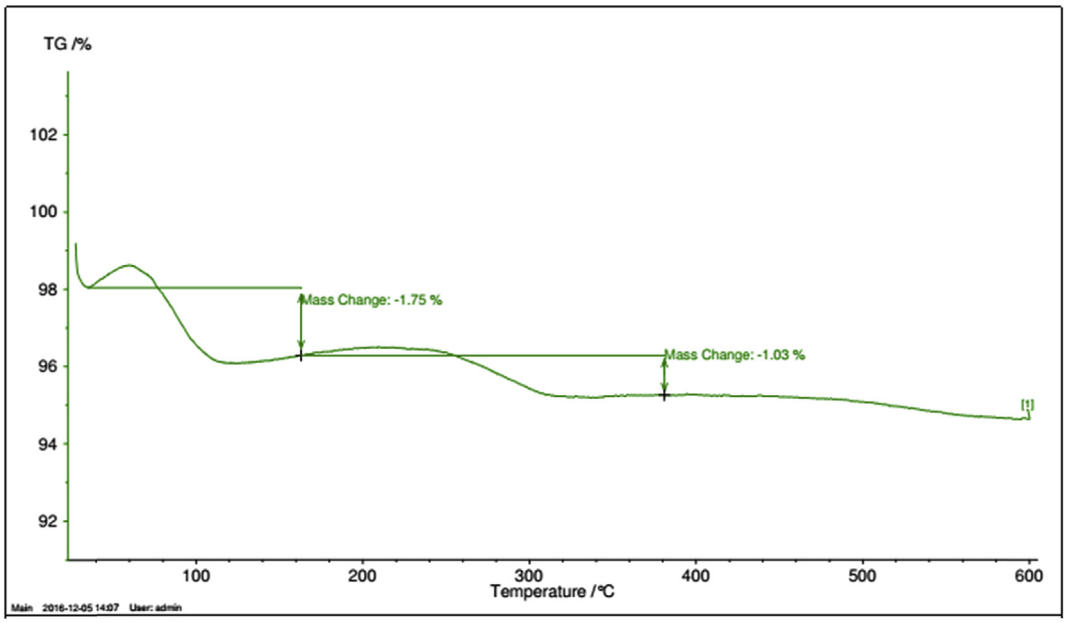

Fig. 3. Thermogravimetric analysis of Fe_3O_4@sepiolite-Pd^{2+}.

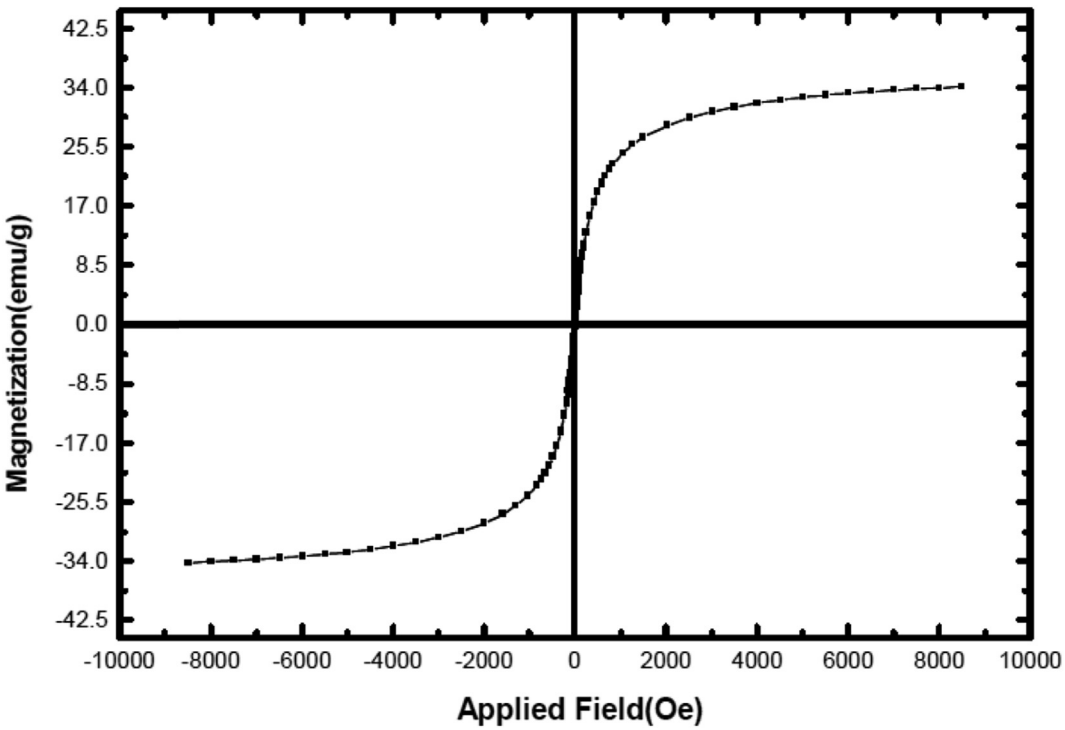

Fig. 4. VSM of Fe_3O_4@sepiolite-Pd^{2+}.

The XRD patterns of two different stepwise synthetic pathways for the preparation of the catalyst are shown in Fig. 6. As compared with sepiolite, the XRD pattern of Fe_3O_4@sepiolite Fig. 6(a) displays five peaks at 30.4°, 35.8°, 43.5°, 54°, 57.5°, and 63.1°, which can be assigned to the characteristic peaks of the cubic magnetite phase. Moreover, the characteristic peaks of sepiolite in the XRD pattern of Fe_3O_4@sepiolite weaken obviously, indicating that the structure of sepiolite may be partly destroyed, resulting in confusional crystal lattice [20].

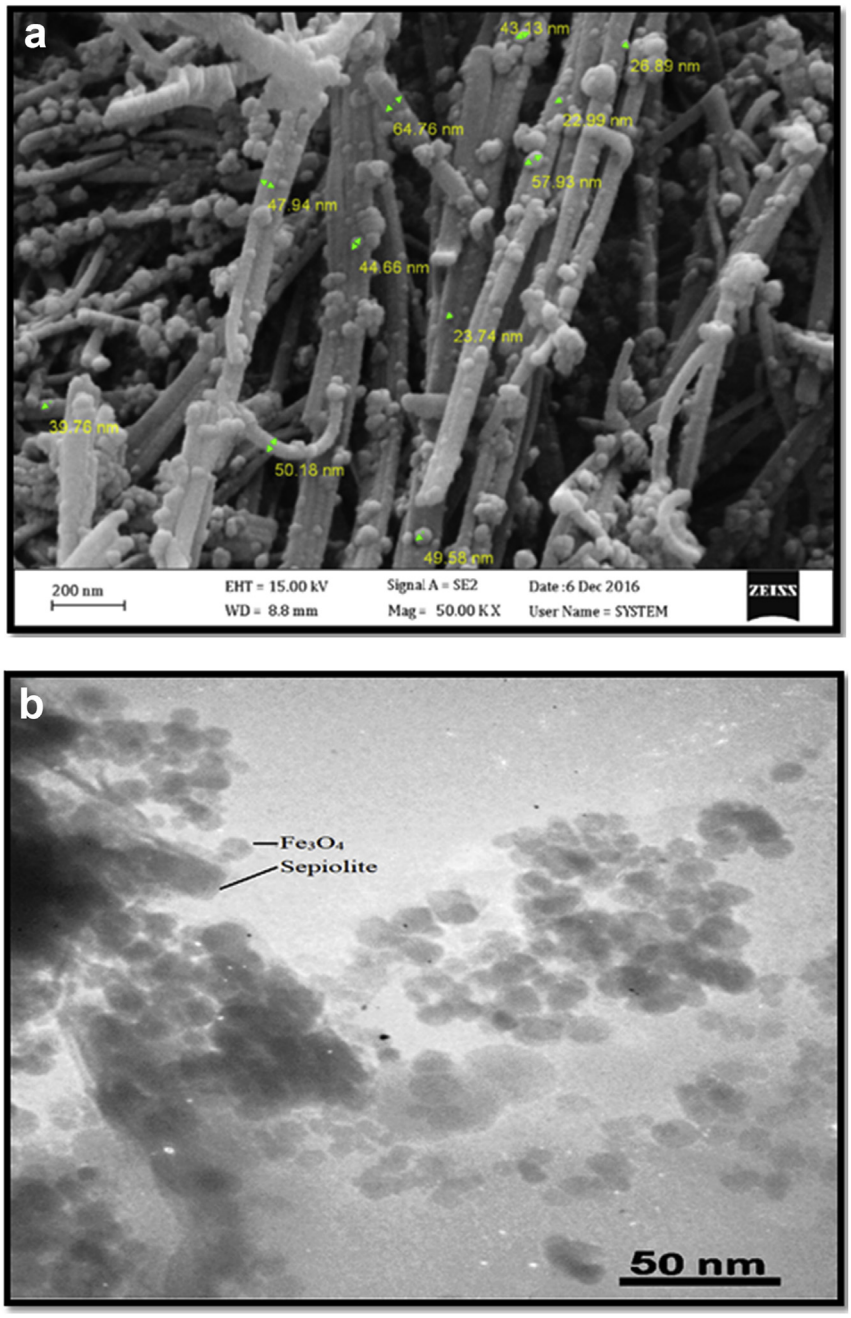

Fig. 5. SEM image of Fe_3O_4@sepiolite-Pd^{2+} (a) and TEM image of Fe_3O_4@sepiolite-Pd^{2+} (b).

The six peaks of Fe_3O_4 can be seen in the XRD pattern of the synthesized Fe_3O_4@sepiolite-Pd^{2+} (Fig. 6(b)). This shows that the prepared Fe_3O_4 nanoparticles in this stage are pure with a spinel structure, and the support of the Fe_3O_4@sepiolite surface with $PdCl_2$ does not result in a phase change of the magnetic nanoparticles. The XRD patterns of the recycled catalyst after two different reactions are shown in Fig. 7. The XRD patterns of the catalyst after the Suzuki reaction Fig. 7(a) show that the catalyst's structure did not change after the reaction, but the XRD patterns of the catalyst after nitro reduction reaction shown in Fig. 7(b) indicate new three peaks around 40.44, 46.54, and 63.11, which, respectively, relate to the (111), (200), and (220) reflections. These peaks confirm the Pd metal in zero oxidation state, indicating the reduction of Pd^{2+} in the presence of $NaBH_4$ as a reduction agent. This change in the nanocatalyst did not reduce its activity [21,22].

The EDX spectrum of the Fe_3O_4@sepiolite-Pd^{2+} catalyst is outlined in Fig. 8. Atoms related to the catalyst structure,

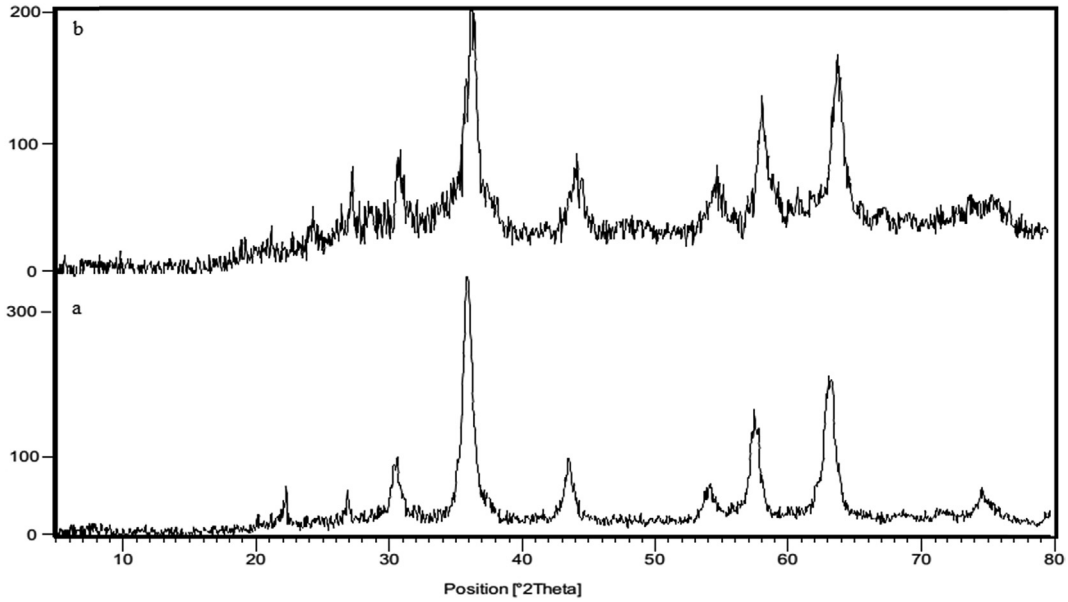

Fig. 6. XRD patterns for Fe_3O_4@sepiolite (a) and Fe_3O_4@sepiolite-Pd^{2+} (b).

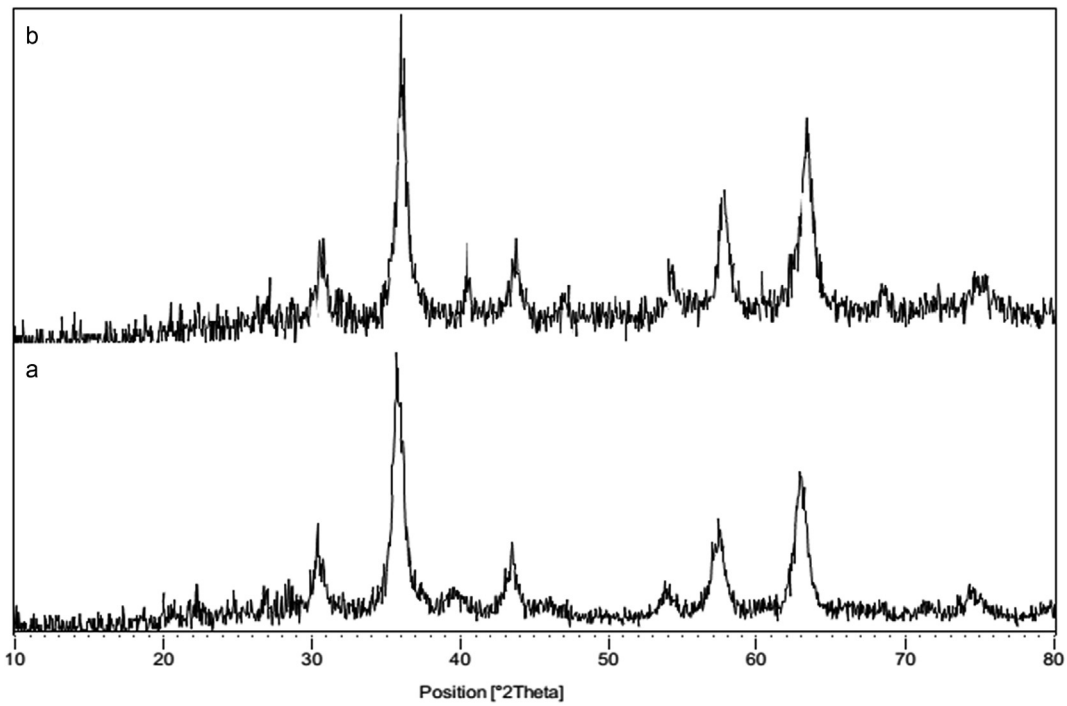

Fig. 7. XRD patterns of nanocatalyst after two reactions: Suzuki reaction (a) and the nitro reduction reaction (b).

such as Fe, Pd, Mg, Al, Si, and O, are seen in this spectrum. The analyses indicated that Pd was coated in the catalyst structure.

After characterization, the activity of the catalyst was tested in both the reduction of nitroarene compounds with $NaBH_4$ and the C–C coupling reaction of phenylboronic acid and aryl halide. First, the reaction of the phenylboronic acid with iodobenzene under various conditions was examined to establish the optimal conditions. The results are summarized in Table 1.

The first reaction was performed under the following conditions: the mixture of phenylboronic acid (1 mmol, 0.122 g) and iodobenzene (1 mmol, 0.204 g) was reacted in the absence of catalyst and 2 mmol (0.276 g) potassium

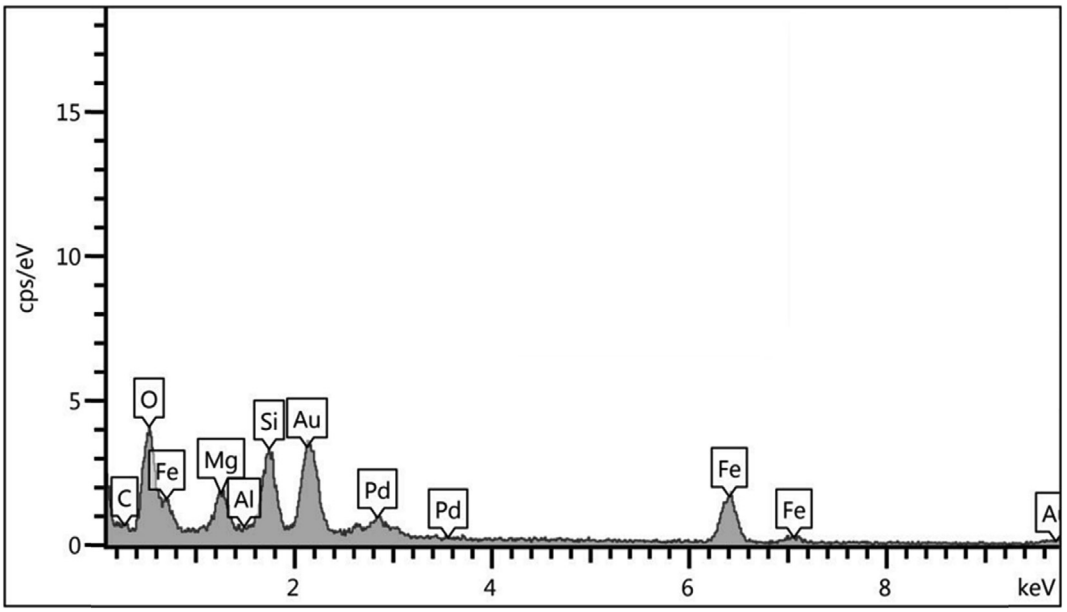

Fig. 8. EDX analysis of Fe_3O_4@sepiolite-Pd^{2+} composite.

Table 1
Characterization of the Suzuki reaction in the presence of different catalysts such as heterogeneous $PdCl_2$.[a]

Entry	Catalyst	Catalyst (mg)	Base	Solvent	Temperature (°C)	Yield[b] (%)
1	–	–	K_2CO_3	EtOH/H_2O (1:1)	45	0
2	Fe_3O_4@sepiolite-Pd^{2+}	5	K_2CO_3	EtOH/H_2O (1:1)	45	43
3	Fe_3O_4@sepiolite-Pd^{2+}	10	K_2CO_3	EtOH/H_2O (1:1)	45	65
4	Fe_3O_4	10	K_2CO_3	EtOH/H_2O (1:1)	45	8
5	Sepiolite	10	K_2CO_3	EtOH/H_2O (1:1)	45	0
6	Fe_3O_4@sepiolite	10	K_2CO_3	EtOH/H_2O (1:1)	45	5
7	Fe_3O_4@sepiolite-Pd^{2+}	10	K_2CO_3	EtOH/H_2O (1:1)	70	95
8	Fe_3O_4@sepiolite-Pd^{2+}	10	K_2CO_3	H_2O	70	10
9	Fe_3O_4@sepiolite-Pd^{2+}	10	K_2CO_3	EtOH/H_2O (2:1)	70	95
10	Fe_3O_4@sepiolite-Pd^{2+}	10	K_2CO_3	EtOH/H_2O (1:2)	70	53
11	Fe_3O_4@sepiolite-Pd^{2+}	10	KOH	EtOH/H_2O (1:1)	70	76
12	Fe_3O_4@sepiolite-Pd^{2+}	10	Na_2CO_3	EtOH/H_2O (1:1)	70	88
13	Fe_3O_4@sepiolite-Pd^{2+}	10	$CaCO_3$	EtOH/H_2O (1:1)	70	12

[a] Phenylboronic acid 1 mmol, iodobenzene 1 mmol, base 2 mmol, catalyst, solvent (8 mL), and 15 min under air atmosphere.
[b] Isolated yield.

carbonate as base in EtOH/H_2O (8 mL, 1:1) at 45 °C under an air atmosphere. After 15 min of reaction time, no product was found. This result showed that the catalyst plays a vital role in this reaction (Table 1, entry 1). To improve yield, 5 mg of Fe_3O_4@sepiolite-Pd^{2+} was used. Yield was increased up to 43%. When the amount of catalyst was increased to 10 mg, the yield was increased up to 65% (Table 1, entry 2–3). The use of Fe_3O_4, sepiolite, and Fe_3O_4@sepiolite as catalyst caused the efficiency of the reaction to decrease to 8%, 0%, and 5%, respectively (Table 1, entries 4–6). The effect of temperature and solvent on the reaction efficiency was also checked. Interestingly, the yield was increased up to 95% when the temperature was increased to 70 °C (Table 1, entry 7). The maximum yield (95%) was obtained when the mixture of EtOH/H_2O (2:1) and (1:1) was used as a solvent; thus, the eco-friendly and greener mixture EtOH/H_2O (1:1) was chosen as the optimal solvent (Table 1, entries 8–10). In addition, the role of different bases was examined; the use of KOH, Na_2CO_3, and $CaCO_3$ instead of K_2CO_3 reduced the yield to 12–88% (Table 1, entries 11–13).

With the optimal conditions determined (Scheme 2), the substrate scope of this reaction was next studied by screening of the aryl halides. A variety of aryl halides were subjected to optimal conditions, and the results are shown in Scheme 2.

All biphenyls products were known and characterized by melting point (mp), IR, and ^1H NMR data as well as by the comparison of their physical data with those in the literature [23–29].

The reduction of nitroarene compounds with sodium borohydride is a powerful synthetic method for the generation of aniline derivatives. In the next section, the catalytic activity of Fe_3O_4@sepiolite-Pd^{2+} for the reduction of

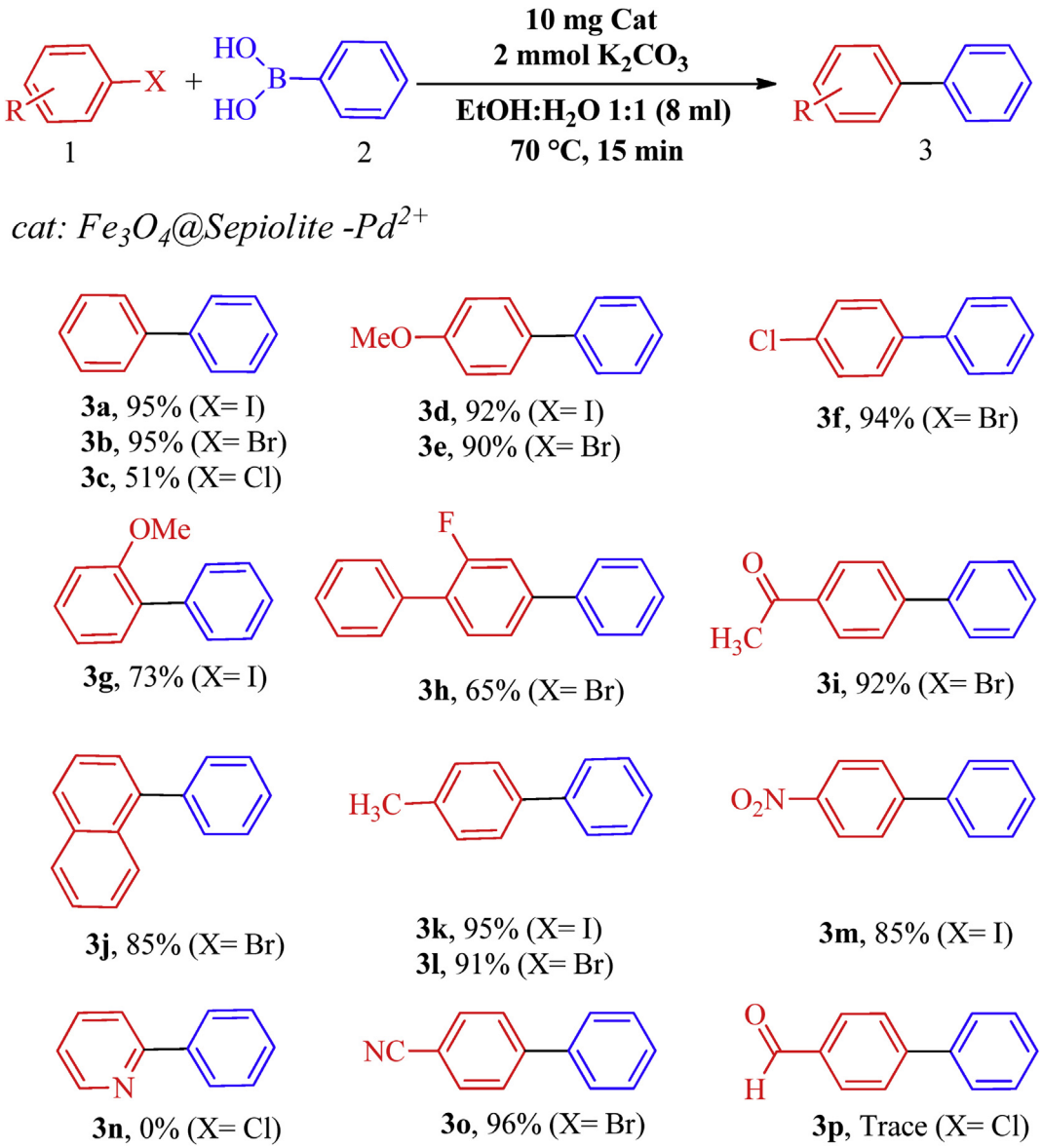

Scheme 2. C-Coupling of various aryl halides (the reactions of aryl halides were carried out on the scale of 1 mmol of aryl halide, 1 mmol phenylboronic acid, 2 mmol K_2CO_3 in 8 mL solvent (EtOH/H_2O 1:1), and in the presence of 10 mg Fe_3O_4@sepiolite-Pd^{2+} at 70 °C for 15 min).

nitroarene compounds is explored. First, the reaction of 2-nitroaniline with $NaBH_4$ under various conditions was examined to establish the optimal conditions. The results are summarized in Table 2.

The first reaction was performed under the following conditions: 2-nitroaniline (1 mmol), $NaBH_4$ as reducing agent (5 mmol), solvent (4 mL), and in the absence of any catalyst at 50 °C under an air atmosphere. After 50 min of reaction time, trace phenylenediamine was found. This result showed that the catalyst played a vital role in this reaction (Table 2, entry 1). To improve yield, 10 mg of Fe_3O_4@sepiolite-Pd^{2+} was used, and the yield was increased up to 45% (Table 2, entry 2). The addition of 10 mg of Fe_3O_4, sepiolite, and Fe_3O_4@sepiolite to the reaction mixture led to only traces of the product, and no catalytic activity for this reaction (Table 2, entries 3–5) took place. In an attempt to improve yield, the effects of both catalyst loading and temperature on the efficiency of the reaction were considered. Interestingly, the yield was increased up to 60% when 20 mg of the catalyst was used (Table 2, entry 6) and up to 96% when the temperature rose to 70 °C (Table 2, entry 7). However, the yield was not changed when an equimolar ratio of EtOH-H_2O (Table 2, entry 8) was used. When the reductant reagent was decreased to 3 mmol, the reaction yield was also reduced to 65% (Table 2, entry 9).

Table 2
Optimization of reaction conditions of reduction of 2-nitroaniline.[a]

Entry	Catalyst	Catalyst (mg)	Solvent	Reductant (mmol)	Temperature (°C)	Yield[b] %
1	–	–	EtOH/H_2O (3:1)	5	50	Trace
2	Fe_3O_4@sepiolite-Pd^{2+}	10	EtOH/H_2O (3:1)	5	50	45
3	Fe_3O_4	10	EtOH/H_2O (3:1)	5	50	Trace
4	Sepiolite	10	EtOH/H_2O (3:1)	5	50	Trace
5	Fe_3O_4@sepiolite	10	EtOH/H_2O (3:1)	5	50	Trace
6	Fe_3O_4@sepiolite-Pd^{2+}	20	EtOH/H_2O (3:1)	5	50	60
7	Fe_3O_4@sepiolite-Pd^{2+}	20	EtOH/H_2O (3:1)	5	70	96
8	Fe_3O_4@sepiolite-Pd^{2+}	20	EtOH/H_2O (2:2)	5	70	93
9	Fe_3O_4@sepiolite-Pd^{2+}	20	EtOH/H_2O (3:1)	3	70	65

[a] Reaction conditions: 2-nitroaniline (1 mmol), $NaBH_4$ as a reducing agent (5 mmol), solvent (4 mL), temperature, 50 min in the presence of a catalyst and under air atmosphere.
[b] Isolated yield.

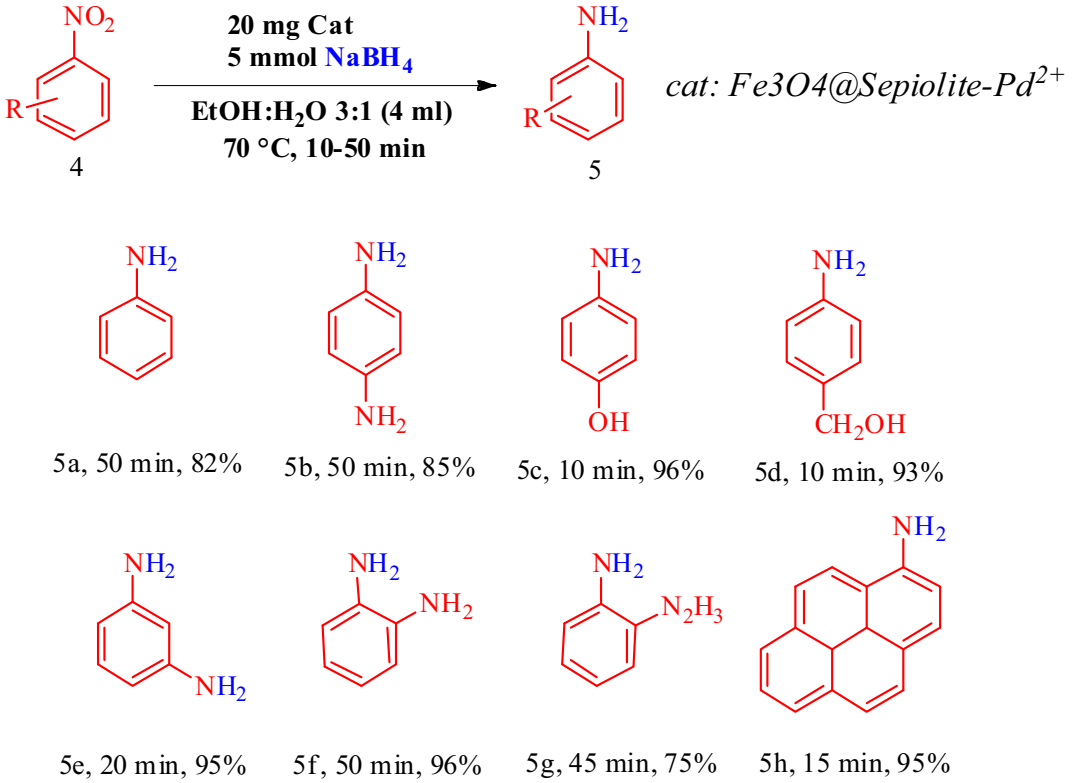

Scheme 3. Reduction of nitroarenes: the reactions of nitroarene were carried out on the scale of nitroarene (1 mmol), $NaBH_4$ 5 mmol (0.189 g), in 4 mL solvent (EtOH/H_2O 3:1), and in the presence of 20 mg Fe_3O_4@sepiolite-Pd^{2+} at 70 °C for 10–50 min, and for the synthesis of **5a**, 10 mmol (0.378 g) of $NaBH_4$ was used.

With the optimal conditions determined (Scheme 3), the substrate scope of this reaction was next studied by screening the nitroarene derivatives. A variety of nitroarenes were subjected to optimal conditions, and the results are depicted in Scheme 3.

All of the nitroarenes were converted to the corresponding anilines in high yields. The corresponding products were known and characterized by IR and ^1H NMR data as well as by the comparison of their physical data with those in the literature [30–34].

The mechanism of the reaction is not entirely clear, but a reasonable mechanism has been depicted in Scheme 4. On the basis of the reaction conditions, the first step of the mechanism was an oxidative addition; Ar-X attached to the catalyst, and an organopalladium compound was formed through a Pd(II)–Pd(IV) catalytic cycle [35]. The next step was transmetalation, and the Ph group was transferred from the activated phenylboronic acid to the palladium catalyst. In the final step of reductive elimination, biaryl was formed and the catalyst was regenerated (Scheme 4).

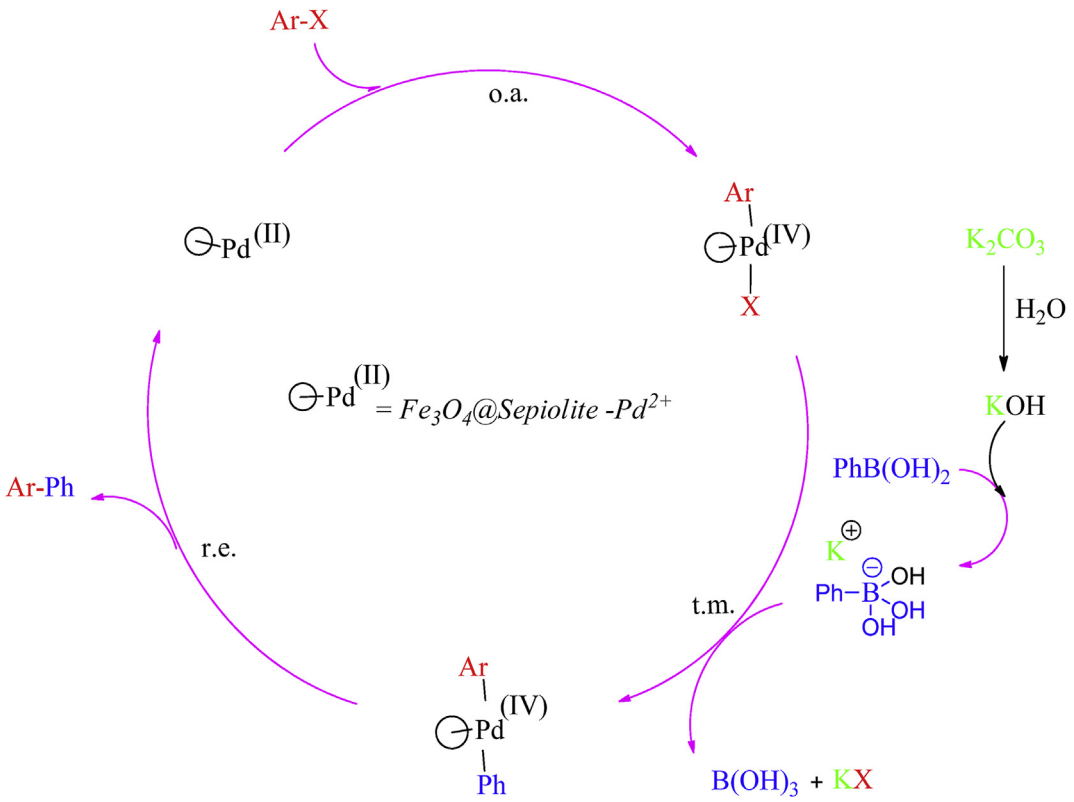

Scheme 4. Proposed reaction mechanism.

Table 3
Comparison of the reaction of bromobenzene with phenylboronic acid (Suzuki coupling reaction) in the presence of nano-Fe_3O_4@sepiolite-Pd^{2+} and some previously reported catalysts.

Catalyst	Temperature (°C)	Time (min)	Yield (%) [ref]
Fe_3O_4@EDTA-Pd^{2+}	80	180	94 [14]
Pd NPs	27	60	95 [36]
Pd/bentonite	25	30	95 [37]
PdCu/RGO	80	30	87 [38]
Fe_3O_4@sepiolite-Pd^{2+}	70	15	95[a]

[a] Present work.

The efficacy of the Fe_3O_4@sepiolite-Pd^{2+} nanoparticles was compared with some previously reported catalysts through the reaction of bromobenzene with phenylboronic acid (see Table 3). The advantages of the catalyst introduced here are a short reaction time, easy separation of the catalyst, and its reusability.

The reusability of the catalyst was tested in the model reaction. After completion of the reaction in the first run, the catalyst was easily separated from the reaction mixture by using an external magnet (Fig. 9(b) and (c)). It was washed twice with ethyl acetate, dried at ambient temperature, and immediately used in the next step. The reaction was repeated for up to five consecutive runs with no significant change in the efficiency of the reaction observed (Fig. 9(a)).

4. Conclusions

In this study, sepiolite clay was used to convert $PdCl_2$ to a heterogeneous catalyst using Fe_3O_4 and characterized as a magnetically separable nanocatalyst. The catalytic activity of the prepared Fe_3O_4@sepiolite-Pd^{2+} was tested in the Suzuki coupling reaction between phenylboronic acid and various aromatic halides in the presence of K_2CO_3 as a base with excellent yields and in short reaction times. Recovery of the catalyst was done using an external magnet. The

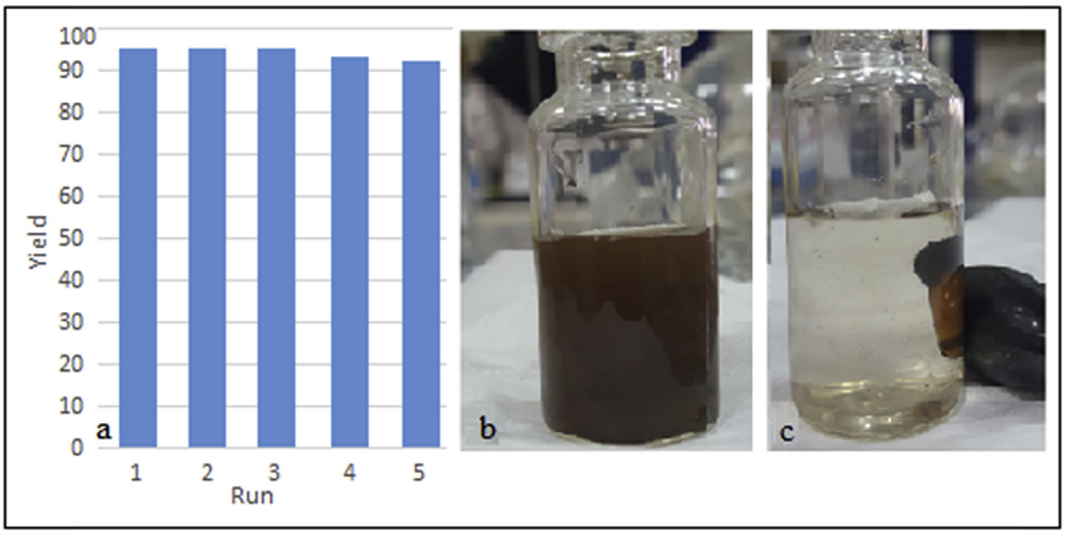

Fig. 9. (a) Reusability of Fe_3O_4@sepiolite-Pd^{2+} in the model reaction; (b) reaction environment during stirring with magnetic bar; and (c) reaction environment after completion of the reaction, nanoparticles adsorbed on the magnetic stirring bar and an external magnet.

catalyst was reused with no significant loss of its catalytic activity. This method was designed based on the principle of green chemistry, avoiding the use of any homogenous or toxic transition metal catalysts.

Acknowledgments

The authors express their appreciation to the Shahid Bahonar University of Kerman for its financial support of this research.

Appendix A. Supplementary data

Supplementary data related to this article can be found at https://doi.org/10.1016/j.crci.2018.07.008.

References

[1] A. Garcia-Sanchez, E. Alvarez-Ayuso, F. Rodriguez-Martin, Clay Miner. 37 (2002) 187.
[2] S. Hashemian, H. Saffari, S. Ragabion, Water Air Soil Pollut. 226 (2015) 2212.
[3] J.M. Diamond, Nature 400 (1999) 120.
[4] S. Guggenheim, R. Martin, Clays Clay Miner. 43 (1995) 255.
[5] S. Lazarević, I. Janković-Častvan, B. Potkonjak, D. Janaćković, R. Petrović, Chem. Eng. Process. 55 (2012) 40.
[6] A. Singer, E. Galan, Developments in Palygorskite-Sepiolite Research: A New Outlook on These Nanomaterials, Elsevier, UK, 2011.
[7] V. Baldoví, A. Corma, H. García, S. Iborra, M.A. Miranda, J. Primo, Recl. Trav. Chim. Pays Bas 111 (1992) 126.
[8] A. Corma, H. Garcıa, A. Leyva, A. Primo, Appl. Catal. A 257 (2004) 77.
[9] P.J. Walsh, H. Li, C.A. de Parrodi, Chem. Rev. 107 (2007) 2503.
[10] P.T. Anastas, J.C. Warner, Green Chemistry: Theory and Practice, 1998, p. 29.
[11] D. Wang, D. Astruc, Chem. Rev. 114 (2014) 6949.
[12] B. Cornils, W.A. Herrmann, Applied Homogeneous Catalysis with Organometallic Compounds, VCH Weinheim, Germany, 1996.
[13] A.K. Gupta, M. Gupta, Biomaterials 26 (2005) 3995.
[14] K. Azizi, E. Ghonchepour, M. Karimi, A. Heydari, Appl. Organomet. Chem. 29 (2015) 187.
[15] R. Liu, Y. Guo, G. Odusote, F. Qu, R.D. Priestley, ACS Appl. Mater. Interfaces 5 (2013) 9167.
[16] A. Tabak, E. Eren, B. Afsin, B. Caglar, J. Hazard. Mater. 161 (2009) 1087.
[17] S. Yu, X. Liu, G. Xu, Y. Qiu, L. Cheng, Desalin. Water Treat. 57 (2016) 16943.
[18] H. Hayashi, R. Otsuka, N. Imai, Am. Miner. 54 (1969) 1613.
[19] K. Naka, A. Narita, H. Tanaka, Y. Chujo, M. Morita, T. Inubushi, I. Nishimura, J. Hiruta, H. Shibayama, M. Koga, Polym. Adv. Technol. 19 (2008) 1421.
[20] S. Starodoubtsev, A. Ryabova, A. Dembo, K. Dembo, I. Aliev, A. Wasserman, A. Khokhlov, Macromolecules 35 (2002) 6362.
[21] Z.-L. Wang, J.-M. Yan, H.-L. Wang, Y. Ping, Q. Jiang, Sci. Rep. 2 (2012) 598.
[22] S. Navaladian, B. Viswanathan, T. Varadarajan, R. Viswanath, Nanoscale Res. Lett. 4 (2009) 181.
[23] D.-H. Lee, J.-H. Kim, B.-H. Jun, H. Kang, J. Park, Y.-S. Lee, Org. Lett. 10 (2008) 1609.
[24] C.-L. Sun, H. Li, D.-G. Yu, M. Yu, X. Zhou, X.-Y. Lu, K. Huang, S.-F. Zheng, B.-J. Li, Z.-J. Shi, Nat. Chem. 2 (2010) 1044.
[25] Ü. Yılmaz, N. Şireci, S. Deniz, H. Küçükbay, Appl. Organomet. Chem. 24 (2010) 414.
[26] D. Zim, A.S. Gruber, G. Ebeling, J. Dupont, A.L. Monteiro, Org. Lett. 2 (2000) 2881.
[27] L. Shen, S. Huang, Y. Nie, F. Lei, Molecules 18 (2013) 1602.
[28] M.E. Hanhan, C. Cetinkaya, M.P. Shaver, Appl. Organomet. Chem. 27 (2013) 570.
[29] Y.L. Zhong, K.P. Loh, A. Midya, Z.-K. Chen, Chem. Mater. 20 (2008) 3137.
[30] J.R. Hwu, F.F. Wong, M.J. Shiao, J. Org. Chem. 57 (1992) 5254.
[31] R. Rajesh, R. Venkatesan, J. Mol. Catal. A Chem. 359 (2012) 88.
[32] I. Pogorelić, M. Filipan-Litvić, S. Merkaš, G. Ljubić, I. Cepanec, M. Litvić, J. Mol. Catal. A Chem. 274 (2007) 202.
[33] E. Ghonchepour, E. Yazdani, D. Saberi, M. Arefi, A. Heydari, Appl. Organomet.Chem. 31 (2017) 3822.
[34] Y.-C. Kung, S.-H. Hsiao, J. Mater. Chem. 20 (2010) 5481.
[35] F. Bellina, A. Carpita, R. Rossi, Synthesis (2004) (2004) 2419.
[36] A. Mahanta, M. Mondal, A.J. Thakur, U. Bora, Tetrahedron Lett. 57 (2016) 3091.
[37] G. Ding, W. Wang, T. Jiang, B. Han, Green Chem. 15 (2013) 3396.
[38] S.J. Hoseini, B. Habib Agahi, Z. Samadi Fard, R. Hashemi Fath, M. Bahrami, Appl. Organomet. Chem. 31 (2017) 3607.